18th Australasian Wind Engineering Society Workshop
McLaren Vale, South Australia
6-8 July 2016

The influence of freestream turbulence on the development of the bluff body shear layer on a square cylinder

D.C. Lander[1], M. Amitay[2] & G.A. Kopp[3], C.W. Letchford[1]

[1]Department of Civil & Environmental Engineering, Rensselaer Polytechnic Institute, Troy, NY, USA

[2]Center for Flow Physics & Control, Department of Mechanical, Nuclear and Aerospace Engineering, Rensselaer Polytechnic Institute, Troy, NY, USA

[3]Boundary Layer Wind Tunnel Laboratory, University of Western Ontario, London, CA

Abstract

The influence of freestream turbulence (FST) on a 2D square prism is investigated at $Re_D = 4.86 \times 10^4$ using long duration Time Resolved Particle Image Velocimetry (TR-PIV). Alterations to flow field in the shear layer and base regions are made and the origins of apparent differences are discussed. Triple-decomposition is employed to identify changes attributable to the to the phase-averaged flow field. In the presence of FST the vortex formation process is altered due to an increase interference of separating shear layers with the trailing edge of the prism which results from an accelerated transition process. This is accompanied by an elongation of the unsteady coherent structures, complementary to the narrowing and elongating of the steady wake, previously observed in the literature.

Introduction

For the better part of a century, scientists and engineers have grappled toward understanding the influence of freestream turbulence (FST) on the aerodynamics of bluff bodies. Yet today, our understanding remains piecemeal and a complete and consistent narrative of the effects of FST on bluff bodies is notably absent. The persistent interest in the topic extends from the pervasiveness of flows where such features are present.

The problem remains unresolved, in part, because the avenues for FST to express its influence are complex, varying and frequently multiscale. For example, where scales of FST match scales of body generated turbulence, perturbations will amplify, attenuate or augment any coherent features of the turbulence. In the case of a square cylinder—an archetype geometry of the tall building—body generated turbulence can be produced from three regions of instability: the attached boundary layer, the separating shear layer and the base/wake region behind the body. Accordingly, there are several domains with difference scales and locations in which disturbances may interact; the properties of the ensuing fluidic structures in these regions are thus dependent on the budget of turbulent energy at the complementary range of the FST, as well as any instantaneous features of the turbulent transition process.

The problem is further confounded by the imposition of the bluff body in the flow field, which accelerates or blocks certain components of the turbulent fluctuations, tilting and stretching the vortical features such that the relative turbulent energy is different to that in its absence. Furthermore, the different regions of instability are often highly inter-dependent. For example, in the wake of the 2D square cylinder, the large scale von-Kármán vortex structures which shed from an absolute-type instability in the base region are contingent on the supply of vorticity from the shear layers, which results from a convective type instability near separation. It follows that cascading effects result from the FST interactions with the different unstable regions; i.e. the interconnected nature of the flow field implies that small disturbances may successively cause alterations to flow features much larger than themselves.

In this study, we focus on problems of this nature, namely, the influence of freestream disturbances which affect the development of the turbulent shear layer separating from the leading edge of a 2D square cylinder. Attention is directed towards the cascading features which arise as a consequence of this interaction, and, in particular, how it alters the formation of the von-Kármán vortex street and the gross aerodynamic loading on the body.

Experiment

Model & Facilities

A 2D square cross-section model (B = D = 76mm) was placed in Tunnel II at the Boundary Layer Wind Tunnel Laboratory at the University of Western Ontario. The Reynolds number was $Re_D = 5.0 \times 10^4$. A small 'rod', 1/10th the size of the main model was placed 45 rod diameters upstream of the body along the stagnation streamline as a means of introducing FST (Case B). This method has been shown to isolate the influence of FST to the shear layers, Gartshore (1973). The intensity of turbulence on the wake centreline was 6.5% and the longitudinal integral length scale was 1/3rd the main body dimension. Cross-stream profiles in the wake of the turbulence generating rod are presented in Fig. 1. It should be noted that measurements in the wake of the rod indicated a broadband turbulent spectra without features of the vortex shedding from the rod itself. These data were compared to those with nominally "smooth" conditions (Case A) i.e. the ambient conditions in the tunnel. Experimental arrangements are illustrated in Fig 2.

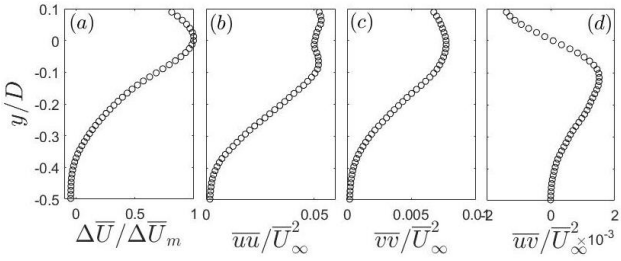

Figure 1. Cross-stream profiles in the wake of the turbulence generating rod. All data are flow components at $x/D = -1.3$ with the model present: (*a*) mean velocity deficit, (*b*) streamwise normal Reynolds stress; (*c*) cross-stream normal Reynolds stress; (*d*) Reynolds shear stress

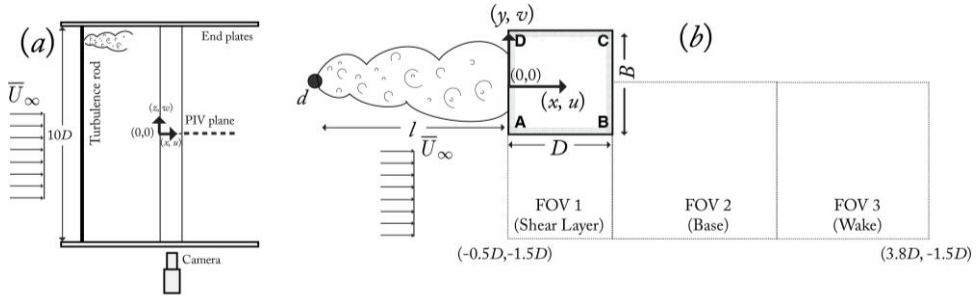

Figure 2. Model arrangements (*a*) plan view; (*b*) sectional view on centreline, here illustrating the relative position of the turbulence generating rod and square cylinder. The three PIV fields of view are shown for the TR-PIV measurement domain taken in the lower half of the wake.

Measurements

Velocity measurements in the lower half of the cylinder wake and unsteady surface pressure measurements around the complete circumference were acquired. Pressures were acquired at a sampling frequency of 1108Hz; simultaneously, Time Resolved-Particle Image Velocimetry data were acquired at a sampling rate of 1000 Hz using a single Photron FASTCAM PCI CMOS camera with 17μm square pixels, 1024×1024 pixel resolution and a 10-bit ADC sensor. This resulted in vector fields resolved at 500 Hz with a spatial range of 1.6D×1.6D, see Fig. 2 (*b*). Seeding particles were atomized olive oil with a mean particle diameter of 1μm while illumination was provided by a double head, diode pumped, Nd:YLF (527μm) Darwin-Duo laser by Quantronix which provided 22mJ/pulse per frame. Cross-correlation of the images was performed using a multi-pass setting of a single-pass 64×64 pixel interrogation window with 50% overlap followed by a dual-pass 32×32 pixel interrogation window with 75% overlap. Post processing smoothed the data in order to eliminate specious vectors, resulting in vector fields contained 128×128 vectors with ~1 vector/mm^2

Analytical treatment

The flow around a square cylinder features large-scale quasi-coherent motions with strong periodicity of von-Kármán vortex structures. With this feature, it is convenient and insightful to decompose the flow into contributions from organised and random motion. Following the notation of Hussain & Reynolds (1972), a flow variable, for example the streamwise velocity, U can be separated according to Eq. (1)

$$U = \overline{U} + u = \overline{U} + \tilde{u} + u' \qquad (1)$$

Where U is the time invariant mean, u is the total fluctuating component which can be separated into; $\tilde{u}$, the contribution of the organised motion and u', the random turbulent fluctuations. Because $\tilde{u}$ is a zero-mean cyclical process intrinsic to the flow, phase locking the time resolved data provides a subset of vector fields with constant phase. For the current experiment with large-scale coherent vortex shedding at $f \sim 17$ Hz, a typical cycle was sampled 29.4 times by the time resolved PIV system. The data were then sorted into 32 discrete phase subsets with each containing approximately 900 images before the phase averaged statistics were determined.

Results

Mean flow field

Fig. 3 presents the mean and rms profiles along the wake centreline along with the results of Lyn *et al*. (1995) and good agreement is observed between the related data. The vortex formation length, L_F, defined as the distance along the wake centreline from the origin to the location of maximum $\sqrt{\overline{vv}}/\overline{U}_\infty$ can be estimated from Fig. 3 (*a*) as $L_{F\{A\}} = 2.21$ and $L_{F\{B\}} = 2.46$ while for Lyn *et al*. (1995), $L_{F\{Lyn\}} = 2.37$. Clearly the effect of FST is to push the wake formation length downstream, decreasing its influence on the base of the cylinder.

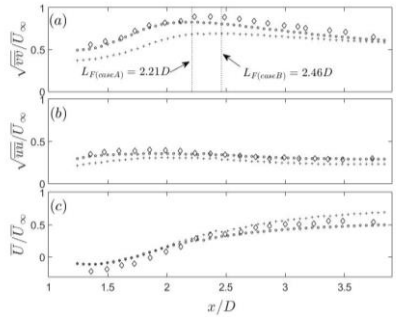

Figure 3: centreline wake profiles of (*a*) rms of cross-stream velocity, (*b*) rms of streamwise velocity, and (c) mean streamwise velocity; ○, case A, present; +, case B, present; ◊, ambient FST ($\sqrt{\overline{uu}}/\overline{U}_\infty$~2%), Lyn *et al*. (1995).

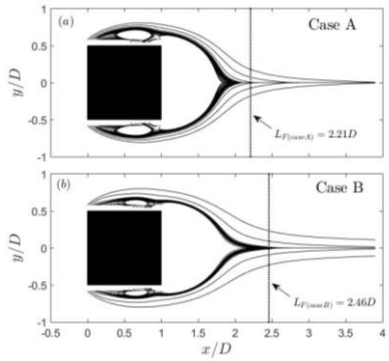

Figure 4: streamlines highlighting the mean base-region (a) case A; (*b*) case B. Also showing vortex formation-length, L_F defined as the distance along the wake centreline from the origin on the front face to the location of maximum $\sqrt{\overline{vv}}/\overline{U}_\infty$, estimated from Fig. 3 (*a*).

Fig. 4 presents time-averaged streamlines originating near the upstream separation corners, (*a*) case A and (*b*) case B. With enhanced FST, the base region has narrowed and elongated slightly while the recirculation regions under the shear layers are reduced in size. Gartshore (1973), hypothesised the addition of FST of sufficient intensity would increase the curvature of the shear layer and cause it to reattach to the body near the leeward corners. The shear layer must subsequently re-separate from the leeward edge, resulting in a straightening of the streamlines in the streamwise direction. These characteristics are consistent with the current results shown in Fig. 4.

The corresponding change in global forces, calculated by integrating the pressures indicate the drag decreased by ~20%; i.e. $C_{D(A)} = 2.35$ while $C_{D(B)} = 1.86$. This is comparable to data presented elsewhere in the literature, Gartshore, (173), Lee (1975). The present results indicate that the reduction in alongwind forces are accompanied by an increase the formation length and a narrowing of the base region. To further understand the origins of these changes and further distinguish the dynamics, the following section present results of the phase averaged flow field.

Phase averaged flow field

In Fig. 5 (facing page) the phase averaged flow field is provided such that the dynamics of the observed changes in the previous section can be observed. Here, the phase averaged vorticity, $\langle\omega_z\rangle^{\phi} = \bar{\omega}_z + \tilde{\omega}_z{}^{\phi}$ is presented over half a period of the von-Kármán cycle. There are several subtle differences between cases (top row is "smooth" (A) while bottom is with added FST (B)) which are noteworthy. For example, the shear layer on the bottom side of the cylinder elongates in the streamwise direction while simultaneously reducing how far it crosses the wake centreline. This results in an apparent elliptical elongation of the von-Kármán vortices. These observations are consistent with the lengthening and narrowing of the wake observed in the mean flow.

To understand the origins of these changes the following sections presents data focused on the development of the bluff body shear layer.

Shear layer development

It was proposed by Gartshore (1973) that FST arriving along the stagnation streamline was responsible for the increased growth of the shear layers due to the rapid distortion of the turbulent eddies arriving alone this trajectory. These ideas can be interrogated directly and are presented in Fig. 6. The shear layer curvature is estimated by $y_c = (\mathrm{d}\overline{U}/\mathrm{d}y)_{max}$, the locus of maximum streamwise velocity gradient at each *x/D*; the shear layer thickness is quantified using the vorticity thickness as $\delta_\omega = \Delta\overline{U}_{max}/(\mathrm{d}\overline{U}/\mathrm{d}y)$ following the work of others Pui & Gartshore (1979), Castro & Haque, (1987).

As can be seen from Fig. 6 (*a*), the increased curvature of the shear layer is significant as predicted. Data of Lyn & Rodi (1994) are also presented and good agreement is seen with the comparable data. Fig. 6 (*b-c*) present the vorticity thickness with downstream distance. It is evident that the growth of the shear layers are approximately linear for both cases, which is similar to planar mixing layers, Brown & Roshko (1974).

In Fig. 6 (*c*) with enhanced FST, the results compare well with that of Castro & Haque (1988) with the trend of decreasing growth rate being consistent between experiments, i.e. decreasing with increasing x/D. It is interesting to note that the shear layer growth rate is not substantially larger in case B, as reported elsewhere & Haque (1988), Pui & Gartshore (1979), Patel (1978). However, the mechanisms through which FST affects the growth rate of the shear layer are complex and still not well understood, Bearman (1983).

In Fig. 7, focusing on the region around the shear layer shortly after separation from the body, a sequence of images from the time-resolved PIV data are shown. Here the *Q-criterion* is used to accentuate the coherent vortices in the shear layer, commonly known as the Kelvin-Helmholtz (KH) vortices. In the case of "smooth" flow Fig. 7 (*a-f*), a typical shear layer transition process is observed. This is characterised by the formation of KH vortices which subsequently pair together before breaking apart into randomly dispersed turbulent eddies. In contrast, in the case with added FST, Fig. 7 (*g-l*), it is apparent that the freestream disturbances have interacted with the KH vortices, causing several to amalgamate into a single larger vortex shortly after separation. The larger vortex has slower convection speed which entrains freestream fluid downstream of itself, toward the side face of the cylinder. This interaction culminates with a blitz of entrained freestream fluid onto the side face, trapping the shear-layer and causing transitory reattachment.

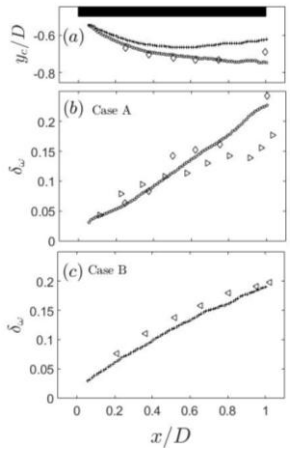

Figure 6: mean properties of the shear layer: (*a*) the location of the centre of the shear layer; (*b*) and (*c*) vorticity thickness, ○, case A, + case B, respectively. Also presented, ◊, Lyn & Rodi (1994); <, enhanced FST; >, ambient FST Castro & Haque (1988)

Conclusions

Flow with ambient levels and enhanced levels of FST have been studied around a 2D square cylinder with an emphasis on understanding the contribution of the shear layer development to altered global aerodynamic characteristics such as drag, base pressure and wake formation length. The PIV data indicated a narrowing and lengthening of the wake; this was accompanied by a rise in base pressure, a reduction in mean drag, and lengthening of the wake formation length. Using triple decomposition, the underlying dynamics of the wake revealed a streamwise lengthening of the individual von-Kármán vortex structures, complementary to the changes observed to the mean wake. Close inspection of the shear layer region indicated a substantial increase in curvature towards the body but no pronounced increase in the shear layer growth rate. Inspection of a series of instantaneous PIV fields of *Q-Criterion* showed that the typical transition pathway, via the formation and subsequent pairing of the KH vortices was bypassed. The KH vortices were observed to cluster and amalgamate after separation before breaking into smaller randomly dispersed cores. The bypass transition was observed to be followed by shear layer reattachment in some cases. This was considered the primary mechanism for the reported changes to the large scale aerodynamic characteristics and the altered wake dynamics.

Acknowledgments

The authors wish to express gratitude to Mr. Abul Fahad Akon and Mr. Gerry Dafoe of the University of Western Ontario and of Mr. Andrew Searle of IO Industries. To Professor Peter Bearman for his insightful comments and stimulating correspondence. To Dr. Reed Cummings for numerous conversations. We also wish to thank Mr. Joesph Baker, Mr. Robert Whiting and Mr. Jordan Fisher for their persistence and dedication as undergraduate researchers on this project. Financial support provided by the National Science Foundation under grant NSF CMMI-1200987.

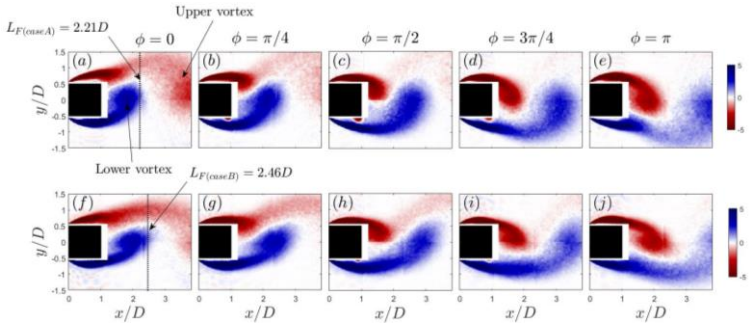

Figure 5: a sequence of phase averaged vorticity showing half a cycle ($\boldsymbol{\phi = 0 - \pi}$) of von-Kármán vortex shedding. Images (*a-e*) are "smooth" flow conditions while *(f-j)* are with increased FST.

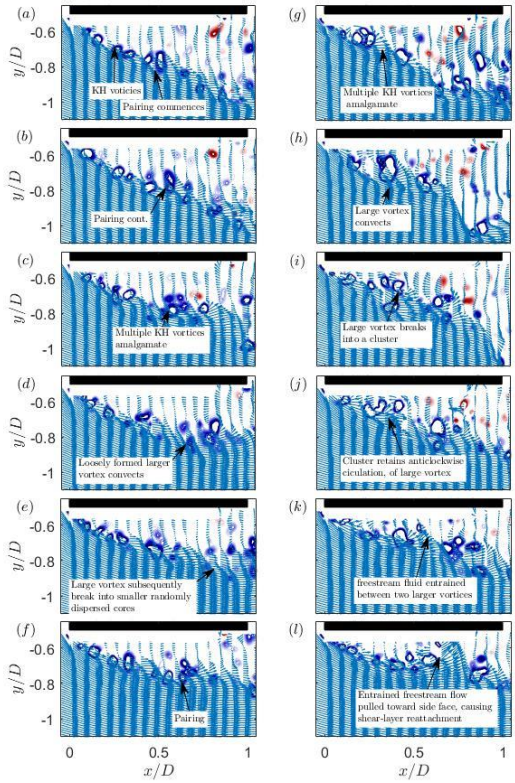

Figure 7: a sequence of consecutive instantaneous flow field images in the shear layer region (black rectangle along top edge represents the lower side of the square cylinder). Here, vectors of velocity are superimposed over contours of *Q-criterion*. Images (*a-f*) are "smooth" flow conditions while *(g-l*) are with increased FST.

References

Bearman, P. W., & Morel, T. (1983). Effect of free stream turbulence on the flow around bluff bodies. *Progress in Aerospace Sciences*, *20*(2-3), 97–123

Brown, G. L., & Roshko, A. (1974). On density effects and large structure in turbulent mixing layers. *Journal of Fluid Mechanics*, 64(04), 775.

Castro, I. P., & Haque, A. (1988). The structure of a shear layer bounding a separation region. Part 2. Effects of free-stream turbulence. *Journal of Fluid Mechanics*, 192(-1), 577.

Gartshore, I. S. (1973). Effects of Free Stream Turbulence on the Drag of Rectangular Two-Dimensional Prisms. *BLWTL report-4-73 UWO*. London, Canada.

Hussain, A. K. M. F., & Reynolds, W. C. (1972). The mechanics of an organized wave in turbulent shear flow. Part 2. Experimental results.*Journal of Fluid Mechanics*.

Lee, B. E. (1975). The effect of turbulence on the surface pressure field of a square prism. *Journal of Fluid Mechanics*, 69(02), 263.

Lyn, D. A., Einav, S., Rodi, W., & Park, J. H. (1995). A laser-Doppler velocimetry study of ensemble-averaged characteristics of the turbulent near wake of a square cylinder. *Journal of Fluid Mechanics*, 304(-1), 285.

Lyn, D. A., & Rodi, W. (1994). The flapping shear layer formed by flow separation from the forward corner of a square cylinder. *Journal of Fluid Mechanics*, 267(-1), 353.

Patel, R. P. (1978). Effects of stream turbulence on free shear flows.*Aeronautical Quarterly*, 29, 33–43.

Pui, N. K., & Gartshore, I. S. (1979). Measurements of the growth rate and structure in plane turbulent mixing layers. *Journal of Fluid Mechanics*,91(01), 111